SPATIAL VARIATIONS IN OVERHEATING RISK OF DWELLINGS UNDER A CHANGING CLIMATE: A CASE STUDY OF SHEFFIELD, UK

Chunde Liu[1], David Coley[2]
[1]University of Bath, Bath, United Kingdom
[2]University of Bath, Bath, United Kingdom

ABSTRACT

As the climate warms, the frequency and scale of extremely hot events are likely to increase. This study predicts overheating risk for the city of Sheffield, UK at a spatial resolution of 5km when the diurnal Urban Heat Island effect is included. Local Hot Summer Years for current and future years are introduced based on the outputs from the UK Climate Projections weather generator. It is found that overheating risk in the urban sites is higher than the adjacent sites and the discrepancy increases with changing climate. Therefore, it is suggested that in general overheating risk is calculated at a high spatial resolution.

INTRODUCTION

In 2003, European countries experienced extremely hot summer, which led to devastating consequences. More than 52,000 people died from heatwave as Earth Policy Institute (EPI) reported (Larsen 2006). According to the report, London experienced the highest temperature on the 10th of August, which caused about 900 heat-related deaths, while in Paris, the daily maximum temperature reached 40°C for many days and 14,800 died from the hot spell. One of the important reasons for the high morbidity and mortality was that buildings failed to protect people against from the extremely hot weather. Due to the long duration of high nocturnal temperatures that lasted in August, the heat exchange between buildings and the outdoor environment was significantly altered (Glenn R McGregor and Gosling 2007). Consequently, residents who were being exposed to the high indoor temperatures were unable to survive. According to the Fifth Assessment Report published by Intergovernmental Panel on Climate Change (IPCC, 2013), it is likely that the global mean surface temperature will be 2.6°C to 4.8°C higher (under high greenhouse gas emissions scenario RCP8.5) at the end of 21st century than the reference period of 1986 to 2005. Although the range of increases in global mean surface temperature is smaller than the value presented by Fourth Assessment Report (IPCC, 2007) which estimated that the likely range would be 2.4°C to 6.4°C under SRES A1FI emission scenario, it is still considerable. Meanwhile, the frequency and duration of heat waves are estimated to increase around late 21st century (IPCC 2013). Therefore, the impact of climate change on overheating risk is expected to be increasingly pronounced.

The main assessment method for estimating overheating risk in buildings is that of simulation using a suitable weather file. In the UK, current and future CIBSE Design Summer Years (DSY) are often used. These are now available for 14 UK sites. The DSY is created from approximately 20 years of weather data and is based on the year with the third warmest mean dry bulb temperature (DryT) during April to September. However, due to the simplicity of this method, there are some obvious shortcomings such as the average problem, distribution problem, solar irradiation problem and missing data problem in the DSY (Jentsch et al. 2013).

Several approaches for new future DSY have been presented in previous work (Watkins *et al.* 2012; Smith and Hanby 2012; Jentsch *et al.* 2008; Eames *et al.* 2010b). The new future DSYs are all created from the weather data generated from UK Climate Projections (UKCP09) weather generator. As each running of UKCP09 weather generator produces 3,000 of possible example years, one hundred DSY can be created. According to the previous work mentioned above, one hundred DSYs were ranked based on the single weather variable. Since the indoor environment is affected by combined effects of thermal related weather variables, in this work we develop a new method where the concept of Physiological Equivalent Temperature (PET) created by Hoppe (Hoppe 1999) is used rather than DryT. PET considers multi-weather variables such as air temperature, wind speed, relative humidity and solar radiation. Our source of weather data is the weather data produced by UKCP09's weather generator. We term these new weather years Hot Summer Years (HSYs).

Results from the Hadley Centre climate model shows that urban factors have an impact on the climate change projections especially for urban areas with high building densities (McCarthy et al. 2009), and as is known that there is strong correlation between the high summer temperature and heat related mortality (Hajat et al. 2007; Armstrong et al. 2010). Thus, there is clearly the need to include the Urban Heat Island (UHI) in the HSY. Unfortunately, the UKCP09 weather generator excludes the effect of

urbanisation, the diurnal UHI has been calculated and incorporated into the HSY for the urban areas.

This study aims to estimate the overheating risk via dynamic thermal comfort simulation considering climate change impacts as well as the UHI effect for Sheffield located in the centre of England, UK. The control (1961 to 1990) and future (i.e. in 2050s and 2080s) HSYs for eighteen UKCP09 (5 km × 5 km) grids have been created and include both urban and non-urban sites. Variations in overheating risk of a bedroom in a naturally ventilated semi-detached house, is then calculated.

METHODOLOGY

Local future hot summer year

The process of local HSYs creation is as follows.

One hundred sets of 30-year hourly weather data under the high emissions scenario (SRES A1FI) for each of three time periods (i.e. control, 2050s and 2080s) are generated for each grid using the UKCP09 weather generator. In these data, there are nine daily weather variables (precipitation, maximum temperature, minimum temperature, sunshine fraction, vapour pressure, relative humidity, direct radiation, diffuse radiation and potential evapotranspiration) and seven hourly weather variables (hourly precipitation, temperature, vapour pressure, relative humidity, sunshine fraction, diffuse radiation and direct radiation) which are fewer than required for thermal comfort simulation. Thus, the missing weather variables such as ground temperature, dew point temperature and cloud cover are calculated according to the equations in CIBSE Guide J (CIBSE 2002). Wind speed and wind direction are calculated based on the method presented by Eames *et al.* (2010a). Then, one DSY can be created from one set of 30-year hourly weather data based on the same method used in the CIBSE DSY. From one hundred sets of 30-year hourly weather data, therefore, one hundred sets of DSY can be obtained.

Second, mean summer PET for each DSY is calculated from the air temperature, wind speed, relative humidity and global solar radiation using RayMan software developed by Meteorological Institute of the University of Freiburg, Germany. As Hoppe (1999) stated, PET is equivalent to the air temperature at which the heat of a standardised person is balanced in a typical indoor environment. The thermo-physiological heat balance model 'Munich Energy Balance Model for Individuals (MEMI)' is the basis for the PET calculation. The DSY with the highest mean summer PET is chosen for HSY.

Third, the mean summer UHI for Sheffield (1.1K) calculated by Kershaw et al. (2010) is downscaled into hourly UHI using the Quarter-sine method developed by Chow and Levermore (2007). Some reasonable assumptions are made in order to construct diurnal UHI. For example, the maximum UHI occurs around the coldest time of the day and minimum UHI occurs around the hottest time of the day (Kershaw *et al.* 2010). In addition, the diurnal variation of the UHI is assumed to have a period of 24 hours. Based on the CIBSE timings (CIBSE Guide A2 Weather & Solar Data, 1982) and the measured UHI (Hathway and Sharples 2012; Lee and Sharples 2008) in Sheffield, it is reasonable to make an assumption that the maximum UHI is 2°C and occurs at 5:00 while the minimum UHI equals 0°C and occurs at 15:00 during all summer. The resultant diurnal UHI created for Sheffield is shown in Figure 1.

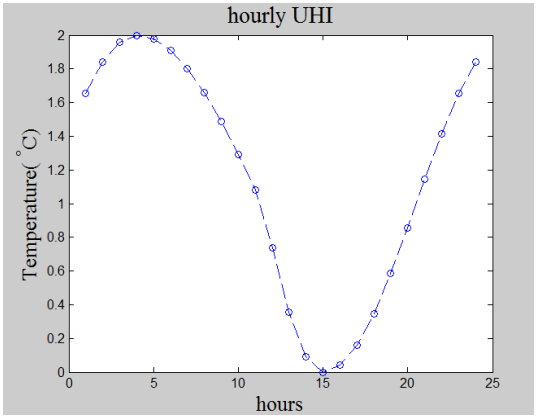

Figure 1 The diurnal variation of the UHI based on the Quarter-sine Method

Last, based on the urban fractions presented by Kershaw et al. (2010), hourly UHI values are incorporated into the HSY for the four grid locations where urban fractions are no less than 0.7 (grid numbers 10, 11, 14 and 15 in Figure 2). The local HSYs in control year, 2050s and 2080s are created for total number of eighteen grids as shown in bottom-right of Figure 2.

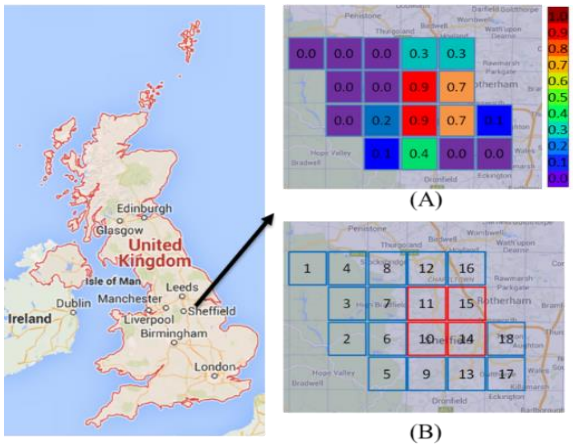

Figure 2 Location and eighteen UKCP09 grids for Sheffield. (A) shows urban fraction of each grid (Kershaw et al. 2010). (B) The four red grids of which urban fractions are no less than 0.7 are considered as urban areas.

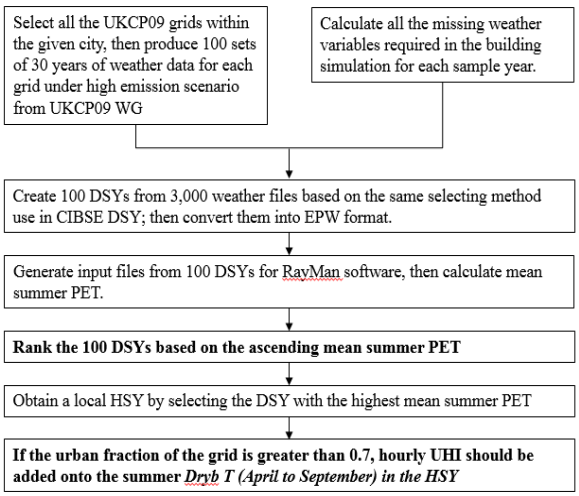

Figure 3 Creation of local HSYs based on the outputs from UKCP09 weather generator and PET.

Thermal comfort simulation

According to the Sheffield Strategic Housing Market Assessment in 2013, the semi-detached house is the most common among the five typical UK dwellings (i.e. semi-detached house, detached house, terraced house, bungalow and flat) in Sheffield and is hence used for thermal modelling. This study used the dimensions, construction and thermal properties of the semi-detached house given in the BEPAC Technical Note 90/2 produced by Allen and Pinney (1990) (who defined standard UK dwellings for building simulations based on the English House Condition Survey) have been assumed. The modelled house is naturally ventilated and the main bedroom in the first floor is facing south so that more solar gains happen than other rooms (see floor plan in Figure 4), and hence represents a worst case scenario. The thermal simulation was carried out using DesignBuilder which contains EnergyPlus as the solution engine. Again, as a worst case, the building is assumed unshaded by any surrounding buildings or trees and the local topography has been ignored. Hence the overheating risk will have been overestimated, however the aim of this study is not the estimation of the exact overheating risk for Sheffield, but the demonstration of the HSY and an investigation as to whether they predict difference risk at such a fine scale (5 km × 5 km).

Overheating risk for this room is examined based on the benchmark summer peak temperature recommended by CIBSE Guide A (CIBSE 2006). This static criterion for overheating risk assessment claims that the percentage of occupied hours ($H_{overheating}$) in a bedroom with the operative temperature above 26°C should not exceed 1 % of annual occupied hours (H_{annual}), i.e. overheating risk (OHR) can be defined as:

$$OHR = \frac{H_{overheating}}{H_{annual}} \times 100\% \qquad (1)$$

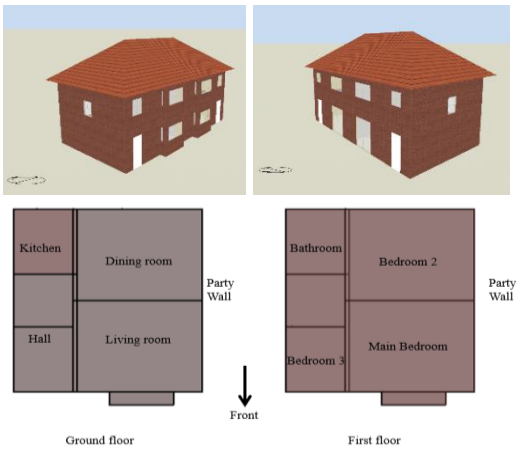

Figure 4 Semi-detached house simulation model and floor plan

RESULTS AND DISCUSSIONS

Variations in outdoor temperatures

Mean summer (April to September) DryT (T_{mean}) of HSY for eighteen UKCP09 grids in control as well as future years under high emission scenario is shown in Figure 5. It can be seen that T_{mean} increases obviously with future scenario, approximately 5°C in 2050s and 8°C in 2080s compared to the control year. In addition, only urban grids (Grid No.:10, 11, 14 and 15) have a T_{mean} exceeding 14°C in the control year. In 2080s, similarly the T_{mean} of each urban grid is apparently higher than 23°C while the values of non-urban grids are not. In 2050s, however, T_{mean} of four urban grids as well as three non-urban grids exceed 19°C. The average absolute differences of T_{mean} between urban and non-urban grids in control year, 2050s and 2080s are approximately 2.3°C, 3.1°C, and 3.4°C respectively. Comparing the urban grids with eastern grids (Grid No.:13, 16 to 18), western grids (Grid No.:1 to 8), northern grids (Grid No.:12 and 16) and southern grids (Grid No.:9 and 13), the absolute differences of T_{mean} are 1.2°C, 3.0°C, 1.5°C, and 1.3°C in control year, while 1.8°C, 4.2°C, 2.8°C, and 1.3°C in 2050s and 2.3°C, 4.1°C, 3.1°C, and 2.5°C in 2080s. Figure 5 also illustrates that the T_{mean} increases as moving eastwards as well as southwards. Furthermore, the average absolute difference of the T_{mean} between western grids and eastern grids is generally greater than the value of northern grids and southern grids for both control and future years.

In order to examine variations of T_{mean} over all grids, coefficient of variations (CV) were calculated based on the equations 2 and 3.

$$CV = \frac{\sigma}{\mu} = \frac{\sqrt{\sum_{i=1}^{N}(T_i - \mu)^2}}{N-1} \times 100\% \qquad (2)$$

$$\mu = \frac{\sum_{i=1}^{N} T_i}{N} \qquad (3)$$

Where, σ is the standard deviation, μ is the average of T_{mean} of all eighteen grids during all summer, N is the total number of grids (i.e. 18) and T_i is T_{mean} of grid number i. The CV of T_{mean} for the control year is 10%, for 2050s 11% and for 2080s 10% are similar, indicating that the climate change has negligible impact on variations CV of T_{mean} across the whole Sheffield.

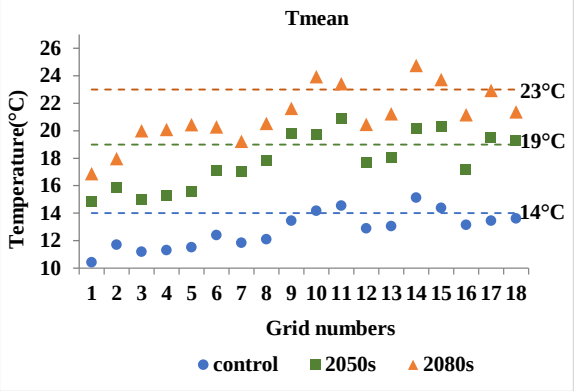

Figure 5 Distribution of T_{mean} across Sheffield during all summer (April to September) in control, 2050s and 2080s. The three dash lines represent 14°C, 19°C and 23°C respectively

The variations of T_{mean} between grids illustrated in Figure 5 arises from the grid weather data offered by the UKCP09 weather generator combined with the method used for creating HSY based on the highest mean summer PET, and the UHI, and we plan to investigate the role of each in later work.

Table 1 shows the grids with the highest and lowest T_{mean} in control, 2050s and 2080s. It can be found that there are big differences between the urban grid with the highest T_{mean} and the non-urban grid with the lowest value in Sheffield. The absolute difference (ΔT) of T_{mean} between the two grids is 4.7°C in control year, 6.0°C in 2050s and 7.8°C in 2080s respectively. For control and 2080s, Grid No.14 shows the highest T_{mean} while in 2050s, the highest value occurs in Grid No.11. Nevertheless, the lowest T_{mean} occurs in Grid No.1 throughout the all of three periods.

Table 1 The largest difference of mean summer Dry T between the eighteen grids

PERIOD	T_{mean} (°C)		
	MAX	MIN	ΔT
cntr	15.1 (Grid No.14)	10.4 (Grid No.1)	4.7
2050s	20.9 (Grid No.11)	14.9 (Grid No.1)	6.0
2080s	24.7 (Grid No.14)	16.9 (Grid No.1)	7.8

The various altitudes of grids no doubt have an impact on T_{mean}. Grid No.1 is lying in the National Park of which altitude is approximately 350 m higher than the urban grids. According to Pepin *et al.* (1999), the environmental laps rate for altitude under 600m is around 2°C/km at nighttime and it rises to around 10°C/km during the daytime in summer. The highly diverse altitudes across the grids could accordingly cause up to a 0.7°C and 3.5°C difference during nighttime and daytime respectively. Integrated into the T_{mean} of the urban grids, the UHI effect might potentially have an impact on the ΔT. Therefore, the high values of ΔT for control and future years shown in Table 1 would be reasonable.

In order to examine the occurrence of the T_{max} and T_{min} above given threshold temperatures, cumulative occurrence P is calculated based on equation (4) as follows.

$$P_{k°C} = \frac{\sum_{j=1}^{D} f(T(j) > k°C)}{D} \times 100\% \qquad (4)$$

Where, P is cumulative occurrence, $P_{k°C}$ is the cumulative occurrence of outdoor temperature i.e. T_{max} or T_{min} above $k°C$ during all summer (April to September), $T(j)$ is outdoor maximum DryT (T_{max}) or outdoor minimum DryT (T_{min}) of day j, f is frequency of outdoor temperature above k°C, k°C is threshold temperature, and D is the total number of days during all summer. ($P_{26°C}$ =13% means that on 13% of days during April to September, the peak outdoor temperatures are above 26°C.).

Figure 6 demonstrates three occurrences i.e. $P_{26°C}$, $P_{28°C}$ *and* $P_{30°C}$ of T_{max} in control and future years. The occurrence is significantly higher in the future than in control year, which is similar to the trend of T_{mean} shown in Figure 5. For T_{max} above 26°C, the $P_{26°C}$ of all grids are lower than 10% except Grid No.11 (13%) and Grid No.14 (12%) in control year. In 2050s, however, the $P_{28°C}$ is higher than 30% except western grids i.e. Grid No.1 to Grid No.6. In 2080s, the $P_{26°C}$ for most of the grids exceeds 50% except several western grids (Grid No.1 to 3 and Grid No.6 to 8). For T_{max} above 28°C and 30°C, $P_{28°C}$ and $P_{30°C}$ for control year are under 5% except Grid No.14 (6%). This suggests that high T_{max} would occur in limited area of the city. For both 2050s and 2080s, on the contrary, most of the grids see $P_{28°C}$ and $P_{30°C}$ significantly higher than 5% except a few western grids. In 2050s, $P_{28°C}$ of western, eastern, southern and northern grids are 14%, 30%, 33% and 20% respectively, while $P_{30°C}$ are 8%, 19%, 20% and 11% respectively. $P_{28°C}$ and $P_{30°C}$ are higher than 25% and 15% respectively in most of the grids except some western and northern grids (i.e. Grid No.12 and Grid No.16). Since around ten grids have high values of $P_{28°C}$ and $P_{30°C}$, more areas would experience a high T_{max} than control year. In 2080s, $P_{28°C}$ of western, eastern, southern and northern grids are 34%, 50%, 43% and 43% respectively, while $P_{30°C}$ are 25%, 42%, 35% and 36% respectively. There would be more days with high T_{max} compared to the days in 2050s since most of the grids see $P_{28°C}$ and $P_{30°C}$ greater than 40% and 30% respectively. Some western grids and one northern

grid (Grid No.12) show the $P_{28°C}$ and $P_{30°C}$ lower than other grids. More importantly, $P_{26°C}$, $P_{28°C}$ *and* $P_{30°C}$ of western grids are generally lower than the values of other grids despite the climate change.

According to the comparison of $P_{28°C}$ and $P_{30°C}$ for both 2050s and 2080s, the high T_{max} occurs more frequently in southern grids than northern ones. Similarly, eastern grids would experience high T_{max} more frequently than western grids. In addition, Figure 6 shows that the difference of T_{max} between urban grids and non-urban grids are not as clear as the difference of T_{mean} in Figure 5. Due to the assumptions of diurnal UHI creation (see Methodology), UHI has been little impact on the T_{max} of urban grids.

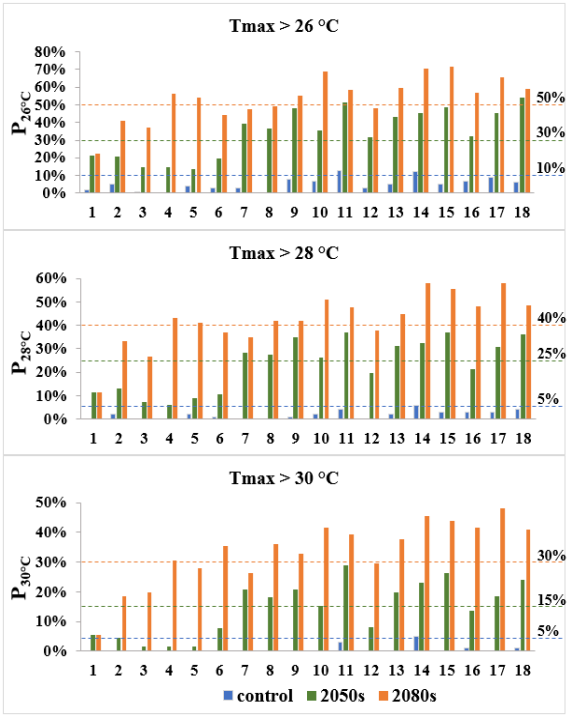

Figure 6 Cumulative occurences of T_{max} above 26°C, 28°C and 30°C during all summer (April to September) in control, 2050s and 2080s.

Figure 7 illustrates $P_{15°C}$, $P_{20°C}$ and $P_{25°C}$ of T_{min} in control and future years. Compared with the control year, as was expected, there will be substantial rise in the occurrence of high T_{min} in the future. For T_{min} above 15°C, $P_{15°C}$ of non-urban grids in control year is under 10% except four urban grids such as Grid No.10 (17%), Grid No.11 (26%), Grid No.14 (32%) and Grid No.15 (20%). In 2050s, $P_{15°C}$ of urban grids are higher than most of non-urban grids. $P_{15°C}$ of western (33%) and northern grids (49%) are apparently lower than eastern (52%) and southern grids (55%). Similarly, in 2080s, $P_{15°C}$ of all urban grids (above 80%) are substantially higher than non-urban grids. Southern parts of urban grids (Grid No.10 and Grid No.14) even have a $P_{15°C}$ greater than 90%. For T_{min} above 20°C, in control year, the $P_{20°C}$ are lower than 5%. The $P_{20°C}$ of urban grids, however, is slightly higher than non-urban grids. In 2050s, $P_{20°C}$ of each urban grid is above 25%, whereas each non-urban grid has a lower value than 25%. $P_{20°C}$ of western, eastern, southern and northern grids are 5%, 11%, 17% and 7% respectively. Thus, it is clear that high T_{min} would occur more frequently in the eastern and southern grids than western and northern grids. In 2080s, $P_{20°C}$ is clearly higher than the one in 2050s across the eighteen grids particularly in urban grids. In addition, there are apparent differences of $P_{20°C}$ between western (19%), eastern (34%), southern (37%) and northern grids (28%). $P_{20°C}$ of urban grids and one eastern grid (Grid No.17) are above 45% that is much higher than the value of other non-urban grids.

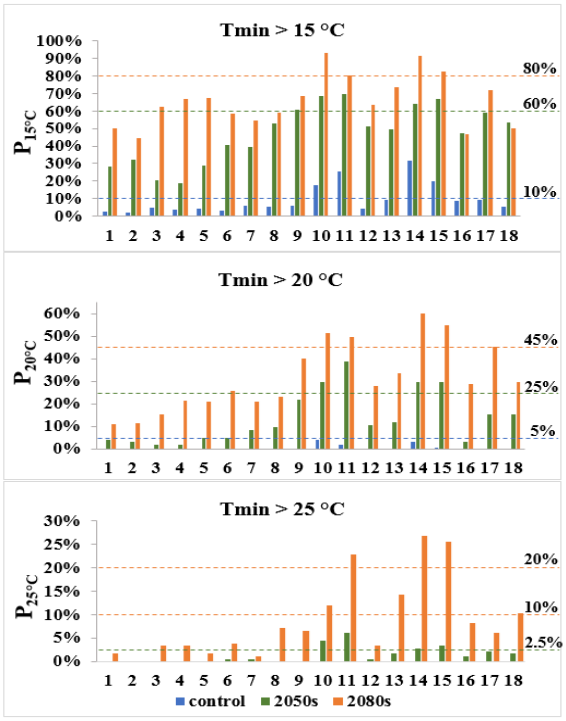

Figure 7 Cumulative occurences of T_{min} above 15°C, 20°C and 25°C during all summer (April to September) in control, 2050s and 2080s

For T_{min} above 25°C, clearly there would be no days with T_{min} above 25°C in control year. In 2050s, $P_{25°C}$ of western grids is approaching zero. $P_{25°C}$ of urban grids are also small, indicating that there would be few summer days with T_{min} above 25°C in 2050s. In 2080s, $P_{25°C}$ of western, eastern, northern and western grids are lower than 10% except the values of Grid No.13 (14%) and Grid No.18 (10%). Nevertheless, there are three urban grids (Grid No.11, Grid No.14 and Grid No.15) with $P_{25°C}$ higher than 20%. This suggests that high nocturnal temperature would occur in 2080s due to a certain period of T_{min} above 25°C during all summer.

According to the assumptions for constructing diurnal UHI (see Methodology), UHI has a greater impact on

the T_{min} than T_{max} of urban grids. By the comparison between urban and non-urban grids, therefore, the difference of P (*i.e.* $P_{15°C}$, $P_{20°C}$ and $P_{25°C}$) of T_{min} is more obvious than the difference of P ($P_{26°C}$, $P_{28°C}$ *and* $P_{30°C}$) of T_{max}. P is projected to rise apparently in the future years because of global warming. Based on the data analysis in terms of four typical directions (western, eastern, southern and northern grids), it could be also found that difference of P between western and eastern grids is greater than the difference between northern and southern grids. The terrain and latitude might be important factors resulting in the difference. Western grids contain part of the national park with high altitude and high density of woods while the eastern grids are adjacent to the urban grids with fewer green spaces. However, the type of terrain of southern grids is similar to the one of northern grids and the difference of latitude between them is small. This indicates that the impact of terrain is greater than the latitude within such a small city. Furthermore, high value of $P_{25°C}$ indicates that high nocturnal temperatures would occur more frequently during summer under future climate scenario. Consequently, there could be dramatic decline in heat exchange between outdoor and indoor environments in the future. It is mentioned in the CIBSE Guide A (CIBSE 2006) that the thermal comfort and sleeping quality would be influenced by high bedroom temperature if it rises above 24°C. Without proper thermal adaption, the dwellings locates in the grid area with high value of $P_{25°C}$ are estimated to be under high risk of overheating in the future.

Variations of indoor overheating risk

A static overheating criterion in CIBSE Guide A (CIBSE 2006) is used for assessing overheating risk in main bedroom (first floor) of semi-detached house. Prior to evaluating variations of *OHR* (see Methodology) across eighteen grids, the effect of UHI on the *OHR* of urban grids has been discussed.

Figure 8 shows the results of the *OHR* from dynamic thermal simulations with and without UHI effect. In control year, *OHR* of all urban grids are below 1%, whereas the *OHR* is projected to rise to above 5% in the future.

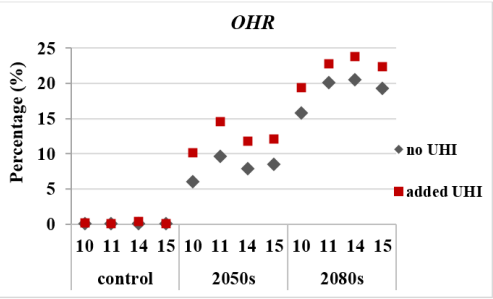

Figure 8 Overheating risk in urban grids with and without diurnal UHI.

There are clear differences between the results with and without UHI effect in 2050s and 2080s. The relative and absolute differences in OHR due to the UHI effect can be calculated based on the following equations.

$$RD = \frac{OHR_{IU} - OHR_{EU}}{OHR_{EU}} \times 100\% \quad (5)$$

$$AD = OHR_{IU} - OHR_{EU} \quad (6)$$

Where, *RD* (%) is relative difference, *AD* is absolute difference, OHR_{IU} is overheating risk with UHI effect while OHR_{EU} is overheating risk without UHI effect.

Without UHI effect, the mean OHR_{EU} of all urban grids in 2050s and 2080s are 8.0% and 18.9% respectively. The values of OHR_{EU} are in the range from 5% to 10% in 2050s. In 2080s, Grid No.14 has the highest OHR_{EU} (20.5%) while Grid No.10 has the lowest OHR_{EU} (15.8%). With UHI effect, the values of OHR_{IU} in 2050s are in the range from 10% to 15%. The *AD* for each urban grid is 4.2%, 4.8%, 4.1% and 3.5% respectively, while *RD* is 70%, 49%, 52% and 40% respectively. In 2080s, *AD* of each urban grid is 3.5%, 2.7%, 3.3% and 3.2% respectively, while *RD* of each grid is 22%, 14%, 16% and 17%.

According to the average *AD* of all grids, there has been steady rise in OHR_{IU} in 2050s (4.1%) and 2080s (3.2%) due to the UHI effect. Moreover, it can be seen that *RD* can be up to 70% in 2050s and 22% in 2080s indicating that UHI might significantly influence the overheating risk in the future.

Figure 9 shows overheating risk of all eighteen grids in control year as well as future years. In control year, the *OHR* in the urban grids are slightly higher than non-urban grids. However, it can be seen that *OHR*s in control year are all under 1%, indicating that overheating would unlikely occur in Sheffield. In contrast, it is estimated that the occupants would suffer serious overheating in the future. In 2050s, for instance, *OHR* exceeds 1% over all grids except three western grids such as Grid No.2(0.9%), Grid No.4(0.6%) and Grid No.5(0.8%). Similar to variations in outdoor temperature, the *OHR* results show that the eastern (6.0%), and southern grids (7.2%) are projected to be at higher overheating risk than western (1.9%) and northern grids (2.8%). In particular, The *OHR* of urban grids are 10.2%, 14.5%, 11.8% and 12.0% respectively which are higher than any other grids. This suggests that these area are more likely to cause overheating. Moreover, it is projected that increasingly severe overheating would occur in 2080s since OHRs are all above 10% except four western grids. The whole city would face overheating problem since the values of OHR in western grids exceed 1%. In addition, the general variations in OHR across the whole grids are similar to the ones in outdoor temperature. For instance, *OHR* of eastern grids (18.5%) is much greater than the one of western grids (10.3%), while *OHR* of southern grids (16.8%) is approximately 1% higher than the one of northern

grids (15.8%). The values of *OHR* in urban grids and one non-urban grid (i.e. Grid No.17) are higher than 19%.

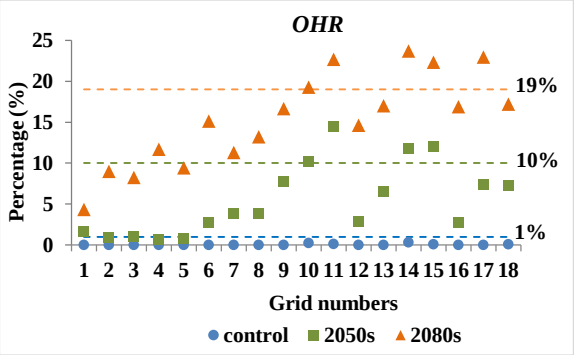

Figure 9 Annual overheating in control, 2050s and 2080s for the main bedroom in the first floor of semi-detached house in Sheffield.

Table 2 reveals the largest absolute difference (ΔOHR) of overheating risk between urban grids and non-urban grids. In general, the maximum OHR occurs in Grid No. 11 and Grid No.14 whereas the minimum OHR is found in the Grid No.1. The results shown in Table 2 is in good agreement with the results shown in Table 1. Thus, it can be inferred that ΔOHR might be strongly related to ΔT. Additionally, ΔOHR for control year, 2050s and 2080s are 0.3%, 13.9% and 19.4% respectively indicating that the occupants would be at substantially high risk of overheating in the future due to the global warming.

Table 2 Maximum and minimum overheating risk in control, 2050s and 2080s

PERIOD	*OHR* (%)		
	MAX	MIN	Δ *OHR*
cntr	0.3 (Grid No.14)	0.00 (Grid No.1)	0.3
2050s	14.5 (Grid No.11)	0.6 (Grid No.1)	13.9
2080s	23.8 (Grid No.14)	4.4 (Grid No.1)	19.4

CONCLUSION

This study presents the variations in overheating risk of Sheffield, UK via dynamic thermal simulation with current and future local HSYs at a spatial resolution of 5 km. In addition, the impact of climate change and UHI effect on overheating risk have been given.

- For the control year, the outdoor temperatures is unlikely to lead to high indoor temperature since T_{mean} across the city is below 14°C (except urban grids) and P of T_{max} and T_{min} above high threshold temperatures are lower than 5%. Consequently, OHR is far below the overheating criterion recommended by CIBSE.
- For future year, the overheating risk is substantially higher than the control year due to the impact of climate change. OHRs of all eighteen grids exceed 1% indicating that even non-urban area of Sheffield would suffer overheating. In addition, OHRs of eastern and southern grids are approximately 4% higher than western and northern grids. In particular, OHR of urban grids are greater than 10% in 2050s and 19% in 2080s respectively suggesting that urban areas would suffer substantial overheating in the future due to the global warming. To sum up, overheating risk is highly diverse across the whole area of Sheffield.
- Due to the UHI effect, OHR_{IU} could be approximately 3% to 4% higher than OHR_{EU} in the future. It can be concluded that the UHI effect would be of importance in assessing overheating risk for the city.

Limitation and future work: the impacts of orientation and thermal properties of the building, occupancy profile were not included in this study; in addition, the assumption when creating diurnal UHI might give rise to some uncertainties for the results. These could be considered as limitations of this study. The future work will pay more attention to the above two aspects. Also, indoor PET and high resolution climate change maps will be investigated in terms of overheating risk.

REFERENCES

Allen, E. & Pinney, A., 1990. Standard dwellings for modelling: details of dimensions, construction and occupancy schedules. Building Environmental Performance Analysis Club Watford, ND.

Larsen, J., Setting the record straight: More than 52,000 Europeans died from heat in summer 20 Washington. DC: Earth Policy Institute, 2006.

Armstrong, B.G., Chalabi, Z., Fenn, B., Hajat, S., Kovats, S., Milojevic, A. & Wilkinson, P., 2010. Association of mortality with high temperatures in a temperate climate: England and Wales. Journal of epidemiology and community health, p. jech. 2009.093161.

Chow, D. & Levermore, G.J., 2007. New algorithm for generating hourly temperature values using daily maximum, minimum and average values from climate models. Building Services Engineering Research and Technology, 28(3), pp. 237-248.

CIBSE, 2002. CIBSE Guide J: Weather, Solar and Illuminance Data. London: The Chartered Institution of Building Services Engineers.

CIBSE, 2006. CIBSE Guide A: Environmental Design. London: The Chartered Institution of Building Services Engineers.

Eames, M., Kershaw, T. & Coley, D., 2010a. The creation of wind speed and direction data for the use in probabilistic future weather files. Building

Services Engineering Research and Technology, 32(2), pp. 143-158.

Eames, M., Kershaw, T. & Coley, D., 2010b. On the creation of future probabilistic design weather years from UKCP09. Building Services Engineering Research and Technology, 32(2), pp. 127-142.

Glenn R McGregor, M.P., Tanja Wolf and & Gosling, S., 2007. Science Report-The social impacts of heat waves. Environment Agency, Rio House, Waterside Drive, Aztec West, Almondsbury, Bristol, BS32 4UD.

Hajat, S., Kovats, R.S. & Lachowycz, K., 2007. Heat-related and cold-related deaths in England and Wales: who is at risk? Occupational and environmental medicine, 64(2), pp. 93-100.

Hathway, E.A. & Sharples, S., 2012. The interaction of rivers and urban form in mitigating the Urban Heat Island effect: A UK case study. Building and Environment, 58(0), pp. 14-22.

Hoppe, P., 1999. The physiological equivalent temperature - a universal index for the biometeorological assessment of the thermal environment. International journal of biometeorology, 43(2), pp. 71-5.

IPCC, 2007. Climate Change 2007: Synthesis Report. Geneva, Switzerland.

IPCC, 2013. Climate Change 2013: The Physical Science Basis. Contribution of Working Group I to the Fifth Assessment Report of the Intergovernmental Panel on Climate Change. Cambridge, United Kingdom and New York, NY, USA: Cambridge University Press.

Jentsch, M.F., Bahaj, A.S. & James, P.A.B., 2008. Climate change future proofing of buildings—Generation and assessment of building simulation weather files. Energy and Buildings, 40(12), pp. 2148-2168.

Jentsch, M.F., Levermore, G.J., Parkinson, J.B. & Eames, M.E., 2013. Limitations of the CIBSE design summer year approach for delivering representative near-extreme summer weather conditions. Building Services Engineering Research and Technology.

Kershaw, T., Sanderson, M., Coley, D. & Eames, M., 2010. Estimation of the urban heat island for UK climate change projections. Building Services Engineering Research and Technology, 31(3), pp. 251-263.

Lee, S. & Sharples, S., Year. An analysis of the urban heat Island of sheffield–the impact of a changing climate. In: PLEA 2008–25th Conference on Passive and Low Energy Architecture, Dublin, October, 2008. pp. 22-24.

McCarthy, M., Best, M. & Betts, R., Year. Cities under a changing climate. In: Paper B9-5, presented at the 7th International Conference on Urban Climate, Yokohama, Japan, 2009.

Pepin, N., Benham, D. & Taylor, K., 1999. Modeling lapse rates in the maritime uplands of northern England: Implications for climate change. Arctic, Antarctic, and Alpine Research, pp. 151-164.

Smith, S.T. & Hanby, V., 2012. Methodologies for the generation of design summer years for building energy simulation using UKCP09 probabilistic climate projections. Building Services Engineering Research and Technology, 33(1), pp. 9-17.

Watkins, R., Levermore, G. & Parkinson, J., 2012. The design reference year - a new approach to testing a building in more extreme weather using UKCP09 projections. Building Services Engineering Research and Technology, 34(2), pp. 165-176.

CIBSE Guide A2 Weather & Solar Data, 1982

Sheffield Strategic Housing Market Assessment, 2013. Available at: http://www.shu.ac.uk/research/cresr/sites/shu.ac.uk/files/sheffield-strategic-hma.pdf [Accessed: 10 May 2014]

UK Climate Projections User Interface, 2012. Available at: http://ukclimateprojections-ui.metoffice.gov.uk/ui/admin/login.php [Accessed: 3 March 2014]